

Identification of asymptomatic vertebral compression fracture using a novel shape-based algorithm

Huy G. Nguyen

University of Technology Sydney

Hoa T. Nguyen

Can Tho University of Medicine

Linh T.T. Nguyen

The 108 Military Central Hospital

Thach S. Tran

University of Technology Sydney

Lan T. Ho-Pham

Ton Duc Thang University

Sai H. Ling

University of Technology Sydney

Tuan V. Nguyen (✉ TuanVan.Nguyen@uts.edu.au)

University of Technology Sydney

Research Article

Keywords: Artificial intelligence, X-ray, Vertebra segmentation, Vertebral fracture, Shape-based Algorithm

Posted Date: March 30th, 2023

DOI: <https://doi.org/10.21203/rs.3.rs-2742621/v1>

License: © ⓘ This work is licensed under a Creative Commons Attribution 4.0 International License.

[Read Full License](#)

Abstract

Background: Vertebral fracture is both common and serious among adults, yet it often goes undiagnosed. The aims of this study were to develop a shape-based algorithm (SBA) for the automatic identification of vertebral fractures.

Results: At the person level, the SBA achieved a sensitivity of 100% and specificity of 61% (95% CI, 51-72%). At the vertebral level, the SBA achieved a sensitivity of 84% (95% CI, 72% to 93%), a specificity of 88% (95% CI, 85% to 90%). On average, the SBA took 0.3 seconds to assess one X-ray.

Conclusions: The SBA developed here is a fast and efficient tool that can be used to systematically screen for asymptomatic vertebral fractures and reduce the workload of healthcare professionals.

Methods: The study included 50 participants whose plain thoracolumbar spine X-rays (n = 144) were taken. Clinical diagnosis of vertebral fracture (grade 0 to 3) was made by rheumatologists using Genant's semiquantitative method. The SBA algorithm was developed to determine the ratio of vertebral body height loss. Based on the ratio, SBA classifies a vertebra into 4 classes: 0=normal, 1=mild fracture, 2=moderate fracture, 3=severe fracture). The concordance between clinical diagnosis and SBA-based classification was assessed at both personal and vertebral levels.

Background

Vertebral fracture is a defining characteristic and a consequence of osteoporosis. The prevalence of vertebral fractures in Caucasian populations is approximately ~ 12% in women and ~ 14% in men (1), with an overall average being 12% for both sexes (2). However, these figures are likely underestimated because the majority of vertebral fractures are asymptomatic (3) and only one-quarter to one-third are clinically recognized (4). More importantly, vertebral fracture is a strong predictor of subsequent risk of non-vertebral fractures and premature mortality (5–7). Collectively, previous data indicate that vertebral fracture is both common and serious among people aged 50 years and older, and this burden is expected to increase in the future as the global population is aging.

Currently, the common method for diagnosing vertebral fractures is to assess X-ray results using Genant's semiquantitative method (8). This diagnosis can be time-consuming and subject to intra-subject reliability. In recent year, artificial intelligence (AI)-related algorithms are a promising approach for identifying vertebral fractures using computer tomography (CT) and to a lesser extent, X-rays (9–14). However, the lack of transparency in these AI algorithms has hindered their widespread adoption in real-world scenarios, as clinicians seek to understand the underlying mechanisms behind their effectiveness in specific situations (15, 16). At least two AI models have been developed to detect vertebral fractures on X-rays. The first model lacked the ability to provide any insights into the functional prognostic of the machine. In the second model, interpretability was added through a workflow that involved vertebra detection, segmentation, and classification of vertebral fractures. This AI model was capable of

predicting vertebral height loss based on the vertebral masks generated by the segmentation module (17–21).

In this study, we used principles of segmentation AI which have been recently adopted in medical image analysis (22) to develop a shape-based algorithm (SBA) as an interpretable AI method for diagnosing asymptomatic vertebral fracture. Our SBA was designed as a rule-based AI to obtain the vertebral corners from a given vertebral mask for measuring the anterior and posterior heights of a vertebra, making the diagnosis of vertebral fracture objective and robust. The present study aimed at quantifying the predictive performance of the SBA in the diagnosis of vertebral fractures on plain X-rays.

Result

The study included 144 participants (106 women) whose average was 55 (standard deviation [SD] 12 years). As expected, individuals with a clinically diagnosed fracture (n = 50) were older than those without a fracture. However, there were no statistically significant differences in weight and height between the two groups (Table 1).

There were 50 individuals who were clinically diagnosed to have a vertebral fracture. Among those with a fracture, the distribution according to severity was as follows: 60% grade 1, 32% grade 2, and 8% grade 3. At the person-level, the sensitivity was 100% (lower 95% CI was 93%) and the specificity was ~62% (95% CI, 51 to 72%). The area under the operating characteristic curve (AUC) value was 0.95 (95% CI, 0.92 to 0.98).

The individuals contributed 1026 vertebrae; of which 57 were clinically diagnosed to have a fracture. Of the 57 clinically diagnosed fractures, the SBA identified 48 fractures (ie sensitivity of 84%). On the other hand, among the 969 non-fracture vertebrae, the SBA algorithm correctly identified 848 (or 88%) as non-fracture. The AUC value for the SBA classification was 0.92 (95% CI, 0.89 to 0.94).

Table 1. Baseline characteristics of 144 individuals stratified by fracture status

	Vertebral fracture (n = 38)	No fracture (n = 460)
Number of women (n; %)	24 (63.2%)	324 (70.2%)
Age (years)	62.7 (12.6)	50.7 (12.3)
Weight (kg)	56.9 (9.3)	55.6 (10.5)
Height (kg)	155 (7.8)	155 (7.4)
Body mass index (kg/m ²)	23.8 (3.6)	23.1 (3.5)
Lumbar spine bone mineral density (g/cm ²)	0.80 (0.14)	0.88 (0.15)

Notes: values are mean (standard deviation) otherwise stated. All individuals did not have a prior non-vertebral fracture. Vertebral fractures were clinically diagnosed using the Genant's criteria.

Table 2. Concordance of the SBA in the grading of vertebral compression fracture compared to rheumatologist-based grading on 1026 vertebrae

SBA classification	Clinical classification			
	Normal (n = 969)	Mild (n = 35)	Moderate (n = 18)	Severe (n = 4)
Normal (n = 857)	848 (87.5%)	5 (14.3%)	4 (22.2%)	0 (0%)
Mild (n = 96)	89 (9.2%)	6 (17.1%)	1 (5.6%)	0 (0%)
Moderate (n = 64)	30 (3.1%)	23 (65.7%)	10 (55.6%)	1 (25.0%)
Severe (n = 6)	2 (0.2%)	1 (2.9%)	3(16.7)	3 (75.0%)

Percent of concordance: 84.5%

Table 3. Concordance between clinically diagnosed vertebral fractures and shape-based algorithm classifications

At the person level

	Clinical diagnosis: Vertebral fracture (n = 50)	Clinical diagnosis: No fracture (n = 94)
SBA Classification		
Fracture	50	36
No fracture	0	58

Percent of concordance = 75%. Sensitivity = 100% (95% CI, 92.9 to 100); Specificity = 61.7% (95% CI, 51.1 to 71.5). Area under the ROC curve: 0.95 (95% CI, 0.92 to 0.98)

At the vertebra level

	Clinical diagnosis: Vertebral fracture (n = 57)	Clinical diagnosis: No fracture (n = 969)
SBA Classification		
Fracture	48	121
No fracture	9	848

Percent of concordance = 87.3%. Sensitivity = 84.2% (95% CI, 72.1 to 92.5); Specificity = 87.5% (95% CI, 85.3 to 89.5). Area under the ROC curve: 0.92 (95% CI, 0.89 to 0.94)

Discussion

Despite the significant morbidity and mortality associated with a vertebral fracture, a large proportion of cases remain undiagnosed, primarily due to its asymptomatic feature. Moreover, the diagnostic process for vertebral fractures is both labor-intensive and time-consuming, and has the potential for bias. In this study, we have created and evaluated a novel AI-based algorithm, known as the 'shape-based algorithm,' for the identification of vertebral fractures. Our findings suggest that the Algorithm can accurately differentiate between individuals with and without fractures, indicating its potential for reducing the workload in daily clinical practice.

Our findings of the performance of SBA are comparable to previous studies' using X-rays. For instance, a study trained a deep convolutional neural network (Visual Recognition V3) on lateral and anteroposterior thoracolumbar spine X-ray to identify vertebral fractures (defined as Genant grades 2 and 3), and this algorithm achieved a sensitivity of 85%, specificity of 87%, and an AUC of 0.91 (12). Another study utilized a multistage model with Random Forest classifier achieved a sensitivity of 74% (13). Collectively, few algorithms had the same prognostic performance as ours. However, our algorithm was faster, taking an average of 35 milliseconds (SD 8) to analyze each vertebra or 312 milliseconds (SD 41) per film compared to the classifier's reported time of 1000 to 2000 milliseconds on a higher-spec CPU (AMD Ryzen 5 3600 CPU, ours: Intel Xeon Gold 6132 CPU).

Our novel method adds to the modest but growing collection of AI tools for vertebral fracture prediction. However, our method was different from previous methods mainly in its interpretability. Indeed, in line with recent trends of interpretable AI, our method promotes the partnership with clinicians (16). We consider that the workflow of our method is transparent, which is often demanded by clinicians.

Our method and findings have important implications in clinical setting. As many vertebral fractures are opportunistic findings, our method can be used for opportunistic screening a large number of X-rays and lessening the burden of clinicians. Moreover, our method, like other AI based methods, can also be used to quickly provide a second opinion to improve the quality of X-ray reports.

However, our findings should be viewed within the context of strengths and potential limitations. The study was designed as a case-control investigation with participants being recruited from the general community, not from clinics where biases could be introduced. The algorithm invented here is not a black box, and clinicians know exactly how the diagnosis is made based on morphometric properties, thereby promoting interaction between doctors and AI methods. Moreover, our method extracts vertebral corners, which extends its application to other morphometric definitions. Nevertheless, a potential weakness was the development and testing in an ideal scenario where the segmentation model achieves doctors' performance. Nevertheless, the difference in practice might be negligible because segmentation models were excellent at drawing out the vertebral body (13, 17–20).

Conclusion

In summary, we have developed and validated a novel shape-based algorithm that is interpretable and can accurately identify asymptomatic vertebral fractures. The algorithm will lessen the workload of clinicians in the assessment of vertebral fractures in high volume settings.

Methods

Vietnam Osteoporosis Study

This study was part of the Vietnam Osteoporosis Study (VOS) in which procedures and protocols have been described in detail elsewhere (23). Briefly, 4157 participants were randomly recruited from the population via advertisement and computer-based selection. We collected the lateral digital X-rays of the spine using the digital X-ray imaging system FCR Capsula XLII (Fujifilm Corp., Tokyo, Japan). The study was approved by the Research and Ethics Committee of People's Hospital 115 and the Pham Ngoc Thach University of Medicine (Ethical approval number 297/BV-NCKH) and carried out according to the relevant guidelines and regulations in compliance with the Declaration of Helsinki. All participants gave their written informed consent. The present study selected 144 individuals from the Study, and the 144 X-rays included 1026 vertebrae for analysis.

Clinical diagnosis by rheumatologists

For each participant, lateral spinal X-ray was taken with a 101.6 cm tube-to-film distance centered at L2, using the FCR Capsula XLII, a high-resolution all-in-one unit with a capacity of up to 50 micrometers reading (Fig. 2). Three rheumatologists read the films independently to diagnose vertebral fracture using the Harry Genant's criteria. Accordingly, a loss of vertebral height of 20–25% was classified as grade 1 (mild); a loss of 25–40% was classified as grade 2 (moderate); a loss greater than 40% was classified as grade 3 (severe). Two rheumatologists visually graded vertebrae from T4 to L4, and any discordance was resolved by a consensus reading with the third and more experienced rheumatologist.

Quantitative assessment by shape-based Algorithm

To create the shape-based algorithm, we began by verifying the accuracy of image processing. A rheumatologist, unaware of the clinical diagnosis, utilized the GU Image Manipulation Program 2 (GIMP 2) to color each X-ray. The vertebral bodies were colored white and the background was colored black. Any osteophytes and vertebrae that were only partially visible in X-ray film were considered part of the background (Fig. 3b).

The resulting information was stored in a binary image or spinal mask for each vertebra from L5 to T4. Because vertebral projections might overlap, which results in unusable segmentation, we stored the film in two spinal masks, each emphasized either superior projection or inferior projection (Supplement Fig. 1). These two masks were then merged for image processing.

Using computer vision techniques, we cropped a vertebral mask from the spinal mask, and subsequently utilized the SBA method to extract the vertebral corners for each cropped mask then measure the anterior height (H_a), posterior height (H_p), and the height loss (ΔH) (Fig. 3c). We categorized vertebral fracture based on their ΔH values according to Genant's classifications (i.e., mild, moderate, and severe), as mentioned earlier.

Design of shape-based algorithm

The SBA was designed to find the vertebral corners from the vertebral mask according to the four-point morphometry of Smith-Bindman (24). The four vertebral corners lie along the vertebral contour, which serves as the boundary separating the black and white regions of the vertebral mask (Fig. 4b). The SBA algorithm includes two processes: the first is extraction of the four potential points on the vertebral contour, and the second is assigning the correct corners.

To extract points, we made the assumption that the corners comprised a quadrilateral area that encompassed the majority of the white region. The four points possessed the following characteristics:

- (1) The first point is the farthest from the centroid of white region (Fig. 4d);
- (2) The second point is the farthest from the first point (Fig. 4e);
- (3) The third point maximized the triangular area formed with the first and second points (Fig. 4f);
- (4) The fourth point maximized the quadrilateral area formed with the other points (Fig. 4g).

After obtaining the four points in sequence, assuming a left-lateral view film, we utilized the following rules to identify the corners:

- (1) The anterior column is identified by selecting the two points closest to the left border, with the anterior top above the anterior-bottom;
- (2) The posterior column is designed by the remaining points, with the posterior-top above the posterior-bottom.

The four corners extracted from the vertebral mask are used to calculate H_a , H_p then ΔH for the morphometric classification of the vertebral compression fracture (Fig. 4h). Height loss is calculated as:

$$\Delta H = \left(1 - \frac{\text{Min}(H_a, H_p)}{\text{Max}(H_a, H_p)} \right) \times 100$$

Based on ΔH , a vertebra was classified as follows: (1) normal if $\Delta H < 20\%$; (2) mild fracture if $20\% \leq \Delta H < 25\%$; moderate fracture if $25\% \leq \Delta H < 40\%$; and severe fracture if $\Delta H \geq 40\%$.

Statistical analysis

We assessed the accuracy of the SBA both on an individual/person level and on a per-vertebra basis. At either person or vertebra level, we estimated the sensitivity (i.e., the proportion of fractures clinically diagnosed that were correctly identified as fractures by the SBA) and specificity (i.e., the proportion of non-fractures clinically diagnosed that were correctly identified as non-fractures by the SBA). We also assessed the AUC and its 95% confidence intervals. The R statistical environment was utilized for all data management and statistical analyses (25).

Abbreviations

SBA: Shape-based Algorithm

AI: Artificial intelligence

CT: Computer tomography

CPU: Central processing unit

GPU: Graphic processing unit

VOS: Vietnam Osteoporosis Study

GIMP 2: GU Image Manipulation Program 2

H_a : Anterior height

H_m : Middle height

H_p : Posterior height

ΔH : Height loss

Declarations

Ethics approval and consent to participate

Not applicable.

Consent for publication

Not applicable

Availability of data and materials

The shape-based algorithm and a tutorial are available in the 12542344/sba repository, [12542344/sba (github.com)].

Competing interests

No potential conflicts of interest relevant to this article were reported.

Funding

Not applicable.

Author contributions

Conceptualization: HGN, TVN, TST

Data Curation: HTN, LTTN, LTHP

Data analysis: HGN, SHL

Writing and Editing: HGN, TVN, TST

Funding: TVN, LTHP

Acknowledgement

This study was funded by a grant to Prof Tuan Van Nguyen from the National Health and Medical Research Council of Australia.

References

1. Waterloo S, Ahmed LA, Center JR, Eisman JA, Morseth B, Nguyen ND, et al. Prevalence of vertebral fractures in women and men in the population-based Tromsø Study. *BMC Musculoskeletal Disorders*. 2012;13(1):3.
2. O'Neill TW, Felsenberg D, Varlow J, Cooper C, Kanis JA, Silman AJ. The prevalence of vertebral deformity in European men and women: The European vertebral osteoporosis study. *Journal of Bone and Mineral Research*. 2009;11(7):1010-8.
3. Greenspan SL, von Stetten E, Emond SK, Jones L, Parker RA. Instant Vertebral Assessment: A Noninvasive Dual X-ray Absorptiometry Technique to Avoid Misclassification and Clinical Mismanagement of Osteoporosis. *Journal of Clinical Densitometry*. 2001;4(4):373-80.
4. Fink HA, Milavetz DL, Palermo L, Nevitt MC, Cauley JA, Genant HK, et al. What Proportion of Incident Radiographic Vertebral Deformities Is Clinically Diagnosed and Vice Versa? *Journal of Bone and Mineral Research*. 2005;20(7):1216-22.
5. Melton Iii LJ, Atkinson EJ, Cooper C, O'Fallon WM, Riggs BL. Vertebral Fractures Predict Subsequent Fractures. *Osteoporosis International*. 1999;10(3):214-21.
6. Hasserijs R, Karlsson MK, Nilsson BE, I, Johnell O. Prevalent vertebral deformities predict increased mortality and increased fracture rate in both men and women: A 10-year population-based study of 598 individuals from the Swedish cohort in the European Vertebral Osteoporosis Study. *Osteoporosis International*. 2003;14(1):61-8.
7. Hasserijs R, Johnell O, Nilsson BE, Thorngren KG, Jonsson K, Mellström D, et al. Hip fracture patients have more vertebral deformities than subjects in population-based studies. *Bone*. 2003;32(2):180-4.
8. Genant HK, Wu CY, Van Kuijk C, Nevitt MC. Vertebral fracture assessment using a semiquantitative technique. *Journal of bone and mineral research*. 1993;8(9):1137-48.
9. Tomita N, Cheung YY, Hassanpour S. Deep neural networks for automatic detection of osteoporotic vertebral fractures on CT scans. *Computers in Biology and Medicine*. 2018;98:8-15.
10. Pisov M, Kondratenko V, Zakharov A, Petraikin A, Gombolevskiy V, Morozov S, et al. Keypoints Localization for Joint Vertebra Detection and Fracture Severity Quantification. Springer International Publishing; 2020. p. 723-32.
11. Nicolaes J, Raeymaeckers S, Robben D, Wilms G, Vandermeulen D, Libanati C, et al. Detection of Vertebral Fractures in CT Using 3D Convolutional Neural Networks. Springer International Publishing; 2020. p. 3-14.
12. Murata K, Endo K, Aihara T, Suzuki H, Sawaji Y, Matsuoka Y, et al. Artificial intelligence for the detection of vertebral fractures on plain spinal radiography. *Sci Rep*. 2020;10(1):20031.
13. Cheng L-W, Chou H-H, Huang K-Y, Hsieh C-C, Chu P-L, Hsieh S-Y, editors. Automated Diagnosis of Vertebral Fractures Using Radiographs and Machine Learning. *Intelligent Computing Theories and Application*; 2022 2022//; Cham: Springer International Publishing.
14. Iyer S, Sowmya A, Blair A, White C, Dawes L, Moses D, editors. A Novel Approach to Vertebral Compression Fracture Detection Using Imitation Learning and Patch Based Convolutional Neural Network 2020 2020: IEEE.

15. Rudin C. Stop explaining black box machine learning models for high stakes decisions and use interpretable models instead. *Nature Machine Intelligence*. 2019;1(5):206-15.
16. Amann J, Vetter D, Blomberg SN, Christensen HC, Coffee M, Gerke S, et al. To explain or not to explain?—Artificial intelligence explainability in clinical decision support systems. *PLOS Digital Health*. 2022;1(2):e0000016.
17. Seo JW, Lim SH, Jeong JG, Kim YJ, Kim KG, Jeon JY. A deep learning algorithm for automated measurement of vertebral body compression from X-ray images. *Scientific Reports*. 2021;11(1).
18. Kim KC, Cho HC, Jang TJ, Choi JM, Seo JK. Automatic detection and segmentation of lumbar vertebrae from X-ray images for compression fracture evaluation. *Comput Methods Programs Biomed*. 2021;200:105833.
19. Lessmann N, Van Ginneken B, De Jong PA, Išgum I. Iterative fully convolutional neural networks for automatic vertebra segmentation and identification. *Medical Image Analysis*. 2019;53:142-55.
20. Sekuboyina A, Kukačka J, Kirschke JS, Menze BH, Valentinič A. Attention-Driven Deep Learning for Pathological Spine Segmentation. Springer International Publishing; 2018. p. 108-19.
21. Chu C, Belavý DL, Armbrecht G, Bansmann M, Felsenberg D, Zheng G. Fully Automatic Localization and Segmentation of 3D Vertebral Bodies from CT/MR Images via a Learning-Based Method. *PLOS ONE*. 2015;10(11):e0143327.
22. Siddique N, Paheding S, Elkin CP, Devabhaktuni V. U-Net and Its Variants for Medical Image Segmentation: A Review of Theory and Applications. *IEEE Access*. 2021;9:82031-57.
23. Ho-Pham LT, Nguyen TV. The Vietnam Osteoporosis Study: Rationale and design. *Osteoporosis and Sarcopenia*. 2017;3(2):90-7.
24. Smith-Bindman R, Cummings SR, Steiger P, Genant HK. A comparison of morphometric definitions of vertebral fracture. *Journal of Bone and Mineral Research*. 1991;6(1):25-34.
25. Team RC. R: A language and environment for statistical computing (Version 4.0. 5)[Computer software]. R Foundation for Statistical Computing. 2021.

Figures

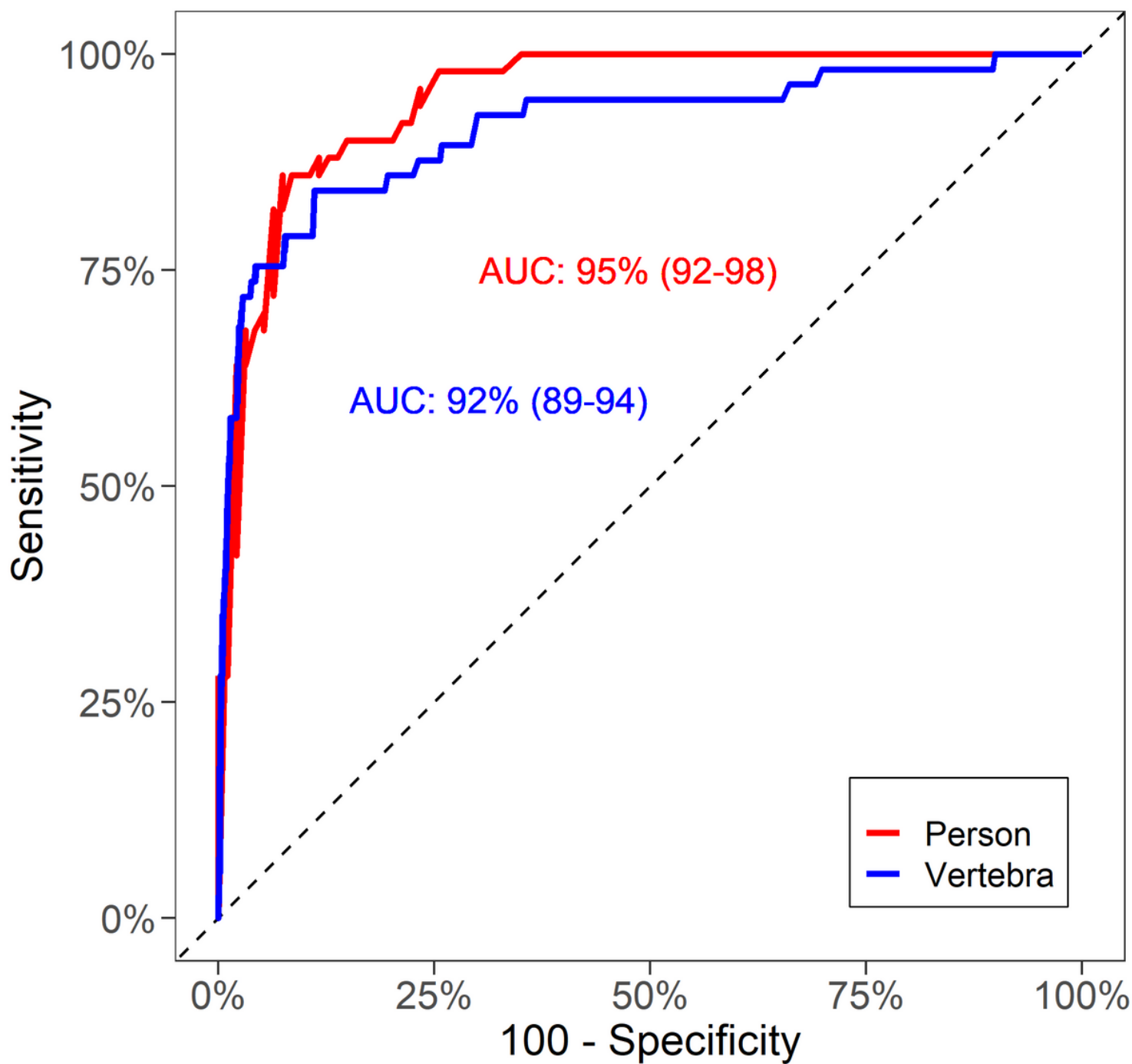


Figure 1

The area under the register operating characteristic curve; The vertebra level is blue, the person level is red; AUCs were presented in percentage and 95% confidence interval.



Figure 2

Representative lateral view plain spine X-ray of a patient with moderate / grade 2 vertebral compression fracture at L1 and mild / grade 1 vertebral compression fracture at T12.

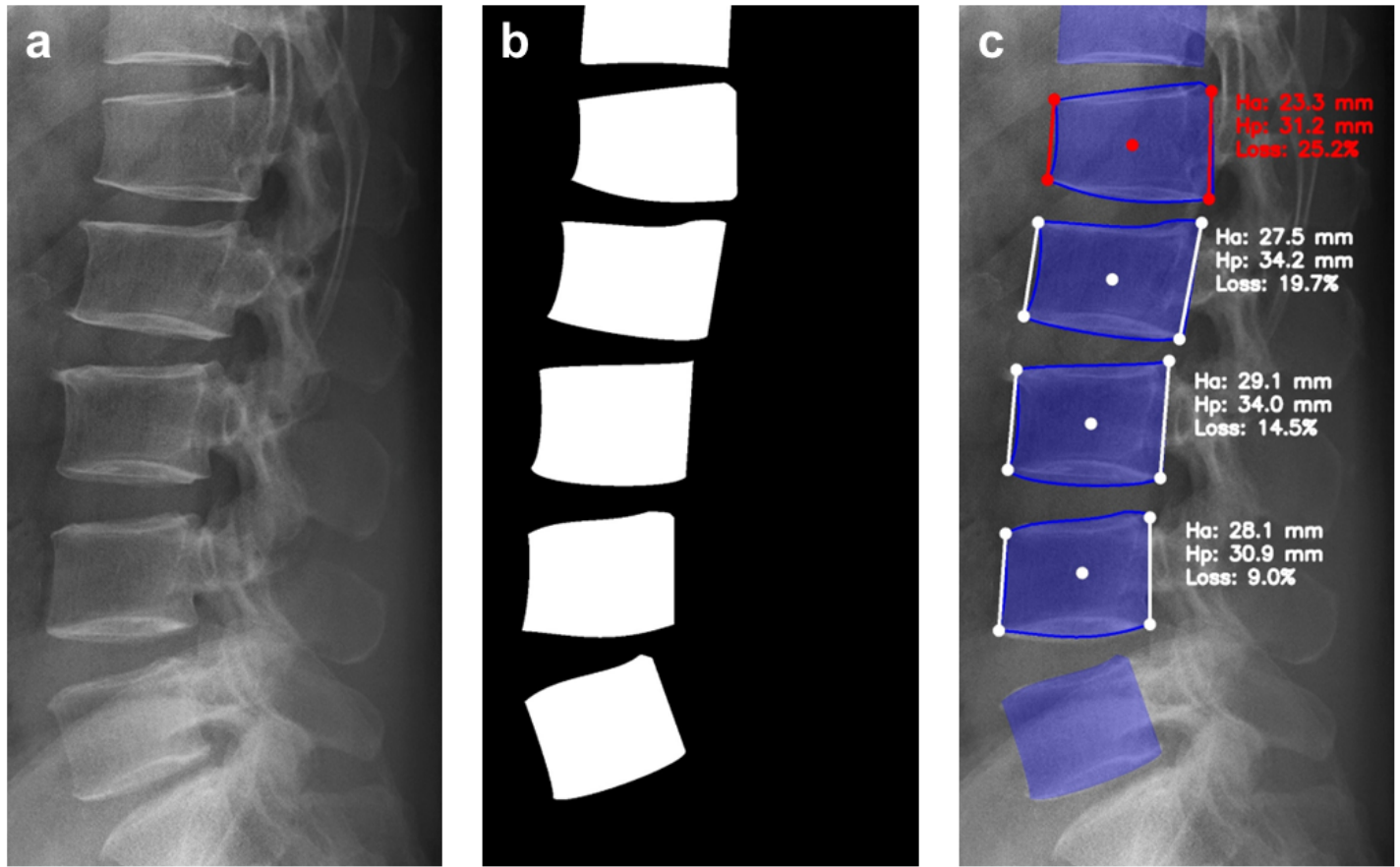


Figure 3

(a) A cropped lumbar spine X-ray from L5 to L1 of a participant; (b) The mask provided by rheumatologists in which the white regions are vertebral bodies and the black region is the background; (c) The shape-based Algorithm extracts the four vertices to calculate vertebral heights in millimeters (Ha: Anterior height; Hp: Posterior height) and height loss in percentage (loss), L1 is moderate / grade 2 vertebral compression fracture with a height loss more than 25%.

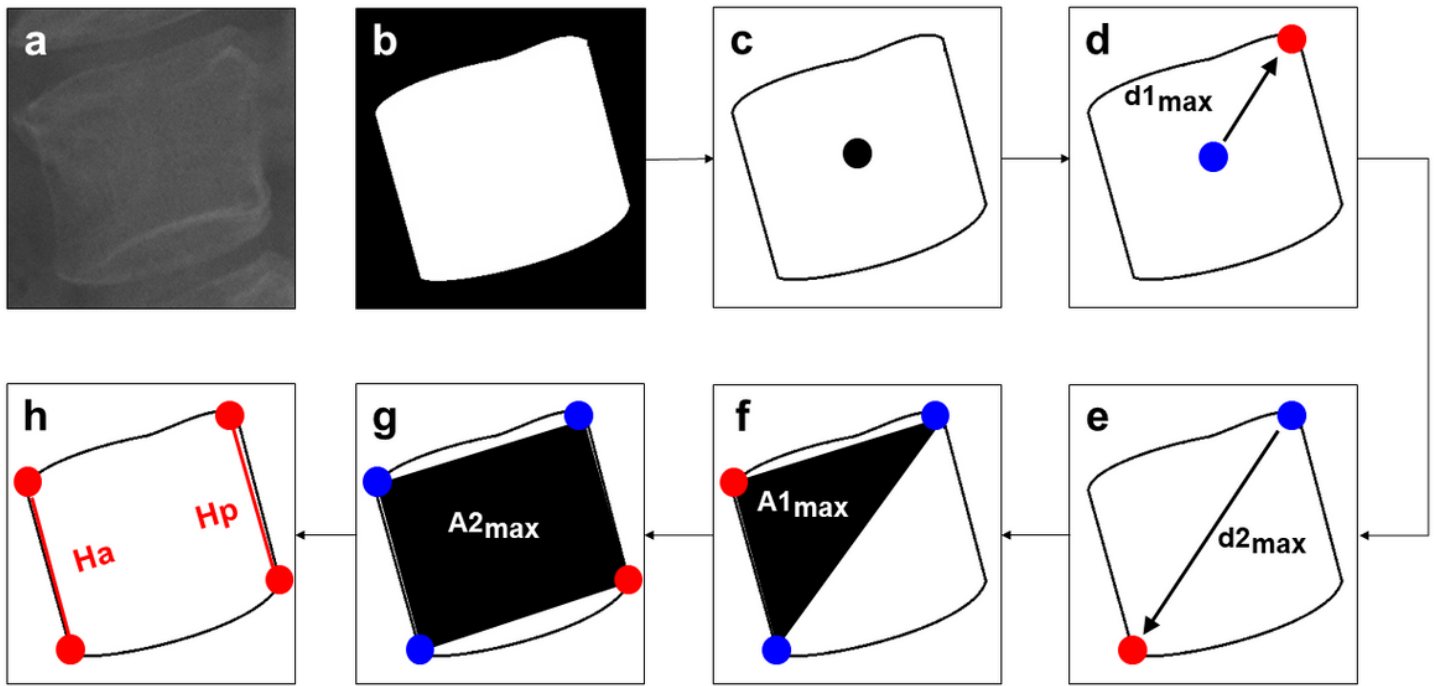


Figure 4

The illustration of shape-based Algorithm. (a) A cropped image of vertebra from a plain lateral spine X-ray; (b) The vertebral mask of the cropped image, black as background and white as vertebral body; (c) The vertebral contour as black line has centroid in black, the task is to identify the four corners with a known contour; (d) The arrow point to the first point in red which is the furthest from the blue centroid; (e) The arrow points to the second point in red which is the furthest point from the first point in blue; (f) The third point in red is chosen to maximize the area formed with found points in blue; (g) The fourth point in red is chosen to maximize the area formed with other points in blue; (h) SBA extracts morphometric properties, two examples are the anterior and posterior height.

Supplementary Files

This is a list of supplementary files associated with this preprint. Click to download.

- [Additionalfigures.docx](#)